Dystrophic Serotonergic Axons in Neurodegenerative Diseases

Efrain C. Azmitia, Ph.D.[a,b] and **Ralph Nixon, Ph.D., M.D.**[b,c]

[a]Department of Biology and Center for Neural Science; 100 Washington Square East; New York, New York 10003

[b]Departments of Psychiatry and Cell Biology, New York School of Medicine, New York, New York 10016

[c]Nathan Kline Institute, Orangeburg, NY 10962

Abstract

Neurodegenerative diseases such as Parkinson's disease (PD), frontal lobe dementia (FLD) and Diffuse Lewy-Body dementia (DLBD) have diverse neuropathologic features. Here we report that serotonin fibers are dystrophic in the brains of individuals with these three diseases. In neuropathologically normal (control) brains (n=3), serotonin axons immunoreactive (IR) with antibodies against the serotonin transporter (5-HTT) protein were widely distributed in cortex (entorhinal and dorsolateral prefrontal), hippocampus and rostral brainstem. 5-HTT-IR fibers of passage appeared thick, smooth, and un-branched in medial forebrain bundle, medial lemniscus and cortex white matter. The terminal branches were fine, highly branched and varicose in substantia nigra, hippocampus and cortical gray matter. In the diseased brains, however, 5-HTT-IR fibers in the forebrain were reduced in number and were frequently bulbous, splayed, tightly clustered and enlarged. Morphometric analysis revealed significant differences in the size distribution of the 5-HTT-IR profiles in dorsolateral prefrontal area between neurodegenerative diseases and controls. Our observations provide direct morphologic evidence for degeneration of human serotonergic axons in the brains of patients with neurodegenerative diseases despite the limited size (n=3 slices for each region (3) from each brain (4), total slices was n=36) and lack of extensive clinical characterization of the analyzed cohort. This is the first report of dystrophic 5-HTT-IR axons in postmortem human tissue

1. INTRODUCTION

The anatomy and plasticity of 5-HT projecting axons in experimental animals has been extensively studied. The fine 5-HT axons were first visualized in the rat brain with histochemical fluorescence (Fuxe 1965). Immunocytochemical analyses with antibodies raised against 5-HT later revealed the full global projections of the raphe neurons, showing also that 5-HT fibers of passage are thick and unbranched while the terminal fibers are fine, highly branched and varicose (Steinbusch 1981; Azmitia and Gannon, 1983). Dense innervation is apparent throughout the neuroaxis and it has been suggested that every cell in the rat cortex is near a 5-HT containing axon (Molliver, 1987).

Corresponding author: Dr. Efrain Azmitia; 10-09 Silver Building; 100 Washington Square East; New York, New York 10003-6688, Office: 212-998-8235; Fax: 212-995-4015; eca1@nyu.edu.

It has been difficult to study the morphology of the 5-HT axonal system in the adult human brain. Postmortem autolysis and the usual methods of postmortem brain fixation result in the loss of 5-HT from axonal storage sites, which makes histochemical fluorescence and 5-HT immunocytochemistry ineffective. Antibodies raised against monoamine hydroxylase enzymes label 5-HT cell bodies and processes in the human brainstem, but fail to reveal the distal terminal fibers (Craven et al, 2005; Underwood et al, 1999; Baker et al, 1991; Haan et al, 1987).

A better approach may be to focus on the 5-HT transporter protein. The 5-HT transporter (5-HTT) protein is specific to 5-HT axons in the adult brain, although occasional astrocytic staining can be observed. The axonal site was visualized in experimental animals by autoradiography after uptake ^{3}H-5-HT by the transporter protein *in situ* (Descarries et al, 1975) or *in vitro* in fresh brain slices (Azmitia, 1981). Antibodies to 5-HTT allowed the morphology of 5-HT terminal axons to be studied immunocytochemically in brains of nonhuman animals (Qian et al, 1995; Zhou et al, 1996). In humans, radioactive ligands specific for the 5-HT transporter permit the gross regional distribution of 5-HT axons to be revealed *in vivo* by PET (Abi-Dargham et al, 1996; Szabo et al, 1996) or in postmortem tissue by film autoradiography (Varnas et al, 2004; Chinaglia et al, 1993). 5-HTT immunoreactive (IR) axons of normal morphology were seen in the postmortem brainstem and prefrontal cortex of individuals without known neurological disorders (Qian et al, 1995; Austin et al, 2001). The 5-HTT-IR axons were described as fine, highly branched and varicose, similar in appearance to those described in non-human animals.

In animal studies, serotonin axons can be damaged under a variety of conditions. Immunocytochemical analysis or immunofluoresence labeling with antibodies raised against 5-HT detects dystrophic immunoreactive fibers in rats after neurotoxic injections ((Wiklund and Bjorklund, 1980; Frankfurt and Azmitia, 1983); ingestion of designer-drugs of abuse (Wilson and Moliver, 1994); and in aged animals (van Luijtelaar et al, 1980). Immunocytochemistry with antibodies to 5-HTT also shows dystrophic 5-HTT immunoreactive axons after neurotoxic injections (Zhou et al, 1996). These dystrophic axons are enlarged, bulbous or splayed after acute damage to 5-HT fibers, suggesting an active degeneration process. In aging animals, 5-HT fibers may appear abnormally fine, varicose and tightly-clustered suggesting atrophy and withdrawal from their forebrain targets (van Luijtelaar et al, 1980).

Despite a preponderance of pharmacological, neurochemical, and molecular evidence that the 5-HT system is disrupted in many clinical disorders, dystrophic serotonergic axons in the human brain have never been described. There is indirect evidence that 5-HT axons are damaged in neurological disorders such as FLD (Sparks and Markesbery, 1991; Menza et al, 1999); PD (Halliday et al, 1990; Marksteiner et al, 2002); Alzheimer's disease and ischemic heart disease (Stout et al 2003); and DLBD (Ballard et al, 2002). For example in DLBD, Lewy bodies occur in the dorsal raphe nucleus, and serotonin levels are markedly reduced in the striatum, neocortex and frontal cortex (Langlais et al, 2003, Ohara et al, 1988; Perry et al, 1993).

In this study, we obtained well-characterized postmortem neurodegenerative brains from patients with PD, FLD and DLBD, as well as from neuropathologically normal (control) individuals. In neuropathologically normal brains, 5-HTT immunocytochemistry showed typical 5-HT axonal morphology in abundant axons, including both projecting fibers and terminating regions, and only rare dystrophic fibers. By contrast, dystrophic 5-HTT-IR fibers were frequent and wide-spread in all brains from patients with degenerative disease. Using a morphometric software system, we identified significant alterations in the number and sizes of 5-HTT-IR axonal structures in the prefrontal terminal regions of all three

neurodegenerative diseases. To our knowledge, this study provides the first direct evidence that 5-HT axons in the human brain are vulnerable to degeneration in neurodegenerative states.

2.0 RESULTS

2.1 5-HTT Patterns in Neuropathologically Normal Brains

5-HTT-IR fibers were seen in all examined regions of neuropathologically normal brains. The 5-HTT-IR axons formed large, dense bundles in the rostral midbrain especially within the medial lemniscus (arrows, Fig. 1A). The 5-HTT-IR fibers of passage were thick, unbranched and either long and straight (possibly myelinated fibers) or wavy in appearance (Fig. 1A).

2.1a. Ascending projections—We observed fine and varicose, or coarse and non-varicose 5-HTT-IR axons in all regions examined. The non-varicose fibers were particularly abundant in brainstem areas associated with major ascending pathways as well as in the forebrain in corpus callosum, fornix, and perforant path fibers The 5-HTT-IR fibers in these forebrain pathways ascended into the gray terminal areas of the cortex where the fibers became thinner and more branched. In addition, a dense fiber plexus of tangential projecting fibers was found in layer I of entorhinal (Fig. 1B) and prefrontal cortical regions (Fig. 1C). These fibers were in close proximity to the pia layer and could be seen extending into layers II and III.

2.1b. Terminal Distribution—In the terminal areas within the midbrain (region of the Substantia Nigra), the 5-HTT antibody labeling resolved thin, varicose, and highly branched 5-HTT-IR axonal fibers. Distinct 5-HTT-IR boutons were visualized at the terminals of these fibers. In entorhinal and prefrontal cortices, the distribution of 5-HTT-IR fibers extended throughout all cortical layers, with extensive branching seen in deeper layers near large pyramidal neurons. The 5-HTT-IR axons were fine, highly branched and formed irregularly spaced varicosities (Fig. 1B–C). The terminals were frequently seen closely surrounding large pyramidal neurons in what can be described as pericellular plexuses.

Occasional dystrophic 5-HTT-IR axons (Fig. 2) were seen in the parahippocampal terminal regions, especially obvious in the oldest brain examined (B3573; male, 79 years of age, postmortem interval of 15.3 hours). The abnormal 5-HTT axons - tight grouping of small varicosities (clustering) (Fig. 2A, arrows) and enlarged varicosities (Fig. 2B–C. arrows) - were scattered among typical fibers, especially in the hilus of the dentate gyrus (Fig. 2B) and the deep entorhinal layers (layer V–VI) (Fig. 2C) and in the CA layers of the hippocampus (not shown). However, there was no evidence in control material of advanced neurodegeneration (splayed endings or dark aggregates of stained material) or a marked reduction in fiber density.

2.2. 5-HTT Patterns in the Brain in Neurodegenerative Diseases

5-HTT-IR axons were found in all regions of brains from individuals with any of the three-neurodegenerative diseases examined. In the brainstem from these cases, 5-HTIR axons appeared normal, although occasional abnormal fibers were seen. Similarly, in the corpus callosum of the forebrain, long 5-HTT-IR axons could be followed with no apparent evidence of pathology, although in the gray matter from this brain region and other cortical gray areas the number of 5-HTT-IR axons appeared markedly reduced. Significant numbers of 5-HTT-IR axons were dystrophic in shape in prefrontal and temporal cortical areas. The hippocampus and entorhinal and prefrontal cortices showed four main types of abnormal profiles: (1) enlarged, twisted and swollen varicosities, sometimes appearing as ballooned

profiles; (2) fine fibers forming tight clusters; (3) isolated splayed fibers with an irregular shape; and (4) densely labeled aggregates and degenerating profiles.

2.3. Diffuse Lewy Body Dementia

In brainstem sections from cases of DLBD, the 5-HTT-IR fibers appeared less dense than normal and occasionally the processes were abnormal in appearance and darkened (arrows, Fig. 3A–B). In both the entorhinal cortex (Fig. 3B–C) and prefrontal (Fig. 3E–F), 5-HTT-IR axons in Layer I, close to the pia, appeared reduced in number. 5-HTT-IR axonal with varicose swelling and ballooning were scattered throughout the cortex and hippocampus. In addition, many 5-HTT-IR axons in the DLBD cortex exhibited clusters of very fine fibers extending from a single process ("splaying") (Fig. 3E).

2.4 Parkinson's Disease

The axonal pathology in Parkinson's patients was severe and seen in all brain regions examined, including the rostral midbrain (Fig. 4). The 5-HTT-IR axonal density appeared to be reduced in all areas, especial the temporal (Fig. 4C–D) and prefrontal (Fig. 4E–F) regions. In brainstem sections from cases of PD (Fig. 4A), the 5-HTT-IR fibers appeared shorter and more fragmented than those seen in neuropathologically normal brains and frequently exhibited enlarged varicosity swellings (Fig. 4B).

In terminal brain areas, 5-HTT fibers exhibit dystrophic morphologies similar to those in DLBD. Layer I showed an apparent reduction in 5-HTT-IR fibers. Dystrophic 5-HTT-IR axons (swollen varicosities) were seen in all regions of the cortical gray matter and in the hippocampus. Many of the 5-HTT-IR axons in the cortex of PD also terminated in the form of clusters of very fine fibers. Enlarged vesicles (Fig. 4C), splayed ending (Fig. 4D), degenerating profile (Fig. 4E) and clustering (Fig. 4F) abnormalities of 5-HTT-IR axons were found in temporal and prefrontal areas.

2.5 Frontal Lobe Dementia

In the brains of patients with FLD, the 5-HTT-IR axonal innervation, especially around the SN, appeared relatively normal although fiber staining was possibly stronger than in neuropathologically normal cases (Fig. 5A–B). Dystrophic axons were infrequent in layer 1 of entorhinal and FLD cortices but were more numerous in the deep layers of prefrontal cortex where they appeared with abnormal swollen varicosities (Fig. 5C, F) clustered (Fig. 5E), splayed and degenerating axons (Fig. 5D), These dystrophic fibers were often seen among normal looking 5-HTT-IR fibers (Fig. 5C, F).

2.6 Morphometric Analysis of Pathologic Changes

Morphometric analyses of the prefrontal cortex region from all cases showed that 5-HTT-IR labeled profiles per unit area were fewer in each group of disease brains than seen in the control brains ($1109+141$ profiles/$0.5mm^2$, n=3). These decreases were statistically significant for the DLBD and Parkinson's diseased brains (FLD-80% of control, n.s.; DLBD-61% of control, $p<.05$.; PD-56% of control, $p < .01$) (Fig. 6A). Typical axons were distinguished from pathological axons by measurements of axon area (Fig. 6B). A histogram of the cross-sectional areas of all 5-HTT-IR profiles for each section (12,233 profiles examined) were measured and expressed as histograms. In control brains, a greater percentage of the total number of profiles (46%) were smaller ($<10\mu2$) than in the disease brain groups (FLD-27%, $p >.05$; DLBD-36%, $p <.01$; PD-37%, n.s.) (Fig. 6B). Conversely, the proportions of large ($30–75\mu^2$) irregular axonal profiles in control brains were lower (24%) compared to the diseased brains (FLD-37%, $p< 0.01$; DLBD-31%, n.s.; PD-31%, n.s.). The differences might be more dramatic and statistically significant if expressed as a

ratio of large to small. Thus computer-assisted morphometric analysis confirmed that the 5-HTT-IR axons in prefrontal cortex from each group of diseased brains were statistically distinct from those labeled in the neuropathologically normal brains.

3.0 DISCUSSION

Our results support previous reports on the immunocytochemical detection of fine 5-HTT axons in human postmortem tissue (Austin et al, 2002; Qian et al, 1995). The 5-HTT-IR axons in postmortem brain sections from individuals without a diagnosed neurological or psychiatric disease were similar to those described previously in humans and animal studies. We detected extensive neuropathology of 5-HTT-IR axons, however, in brains of patients with Parkinson's disease, Frontal Lobe Dementia or Diffuse Lewy-Body Dementia. This is the first report of 5-HT axonal pathology in humans and shows that the 5-HT system in the human brain is vulnerable to degeneration in various neurodegenerative disorders, as shown previously in animal models of disease.

3.1. Serotonin System and Neurodegeneration

Although numerous pathologies in late–age onset neurodegenerative diseases have been identified with markers of specific pathologies (eg. β-amyloid, ubiquitin, hyperphosphorylated-tau or α-synuclein reactive), there are relatively few examples of a transmitter-specific neuronal degeneration in neurodegenerative diseases (see reports on acetylcholine: Bossy-Wetzel et al, 2004, Perry et al, 1993 and norepinephrine: Haglund et al., 2006). Even in Parkinson's diseases, we could not find a description of dystrophic dopaminergic fibers (see Dickson et al, 1994) although the normal distribution of projections from dopaminergic neurons to the human caudate has been described (Kung et al, 1998).

We now report that serotonin fibers, immunocytochemically labeled with antibody against the 5-HTT, show extensive and wide-spread pathology in the brains of patients with PD, FLD or DLBD. In animal studies, serotonin fibers degenerate when exposed to a variety of environmental and neurotoxic factors (e.g. Van Luijtelaar et al, 1989-aging; O'Hearn et al, 1990-MDMA and related drugs; Zhou et al, 1994-alcohol; Liu and Nakamura, 2006; Azmitia et al, 1990-stress hormones; Aucoin et al 2005 amyloid; Baumgarten and Bjorklund, 1976; Frankfurt and Azmitia, 1984–5,7-DHT). Our findings demonstrate that human serotonin axons are also vulnerable to degeneration in pathological states.

3.2 Comparison of Axonal Pathology

Depletion of normal fibers and appearance of degenerating profiles were evident in all three groups of brains from patients with degenerative diseases. There was no evidence that gender or postmortem interval contributed to these observations. Recent unpublished work using 5-HTT immunostaining (n=22 brains from neurologically typical normal subjects, range 32–85 yrs, average age 57.2 yrs. and n=3 female) showed no evidence of the frequent severe 5-HTT-specific axonal pathology reported here in the brains from patients with neurodegenerative diseases. The 5-HTT-IR dystrophic axonal profiles in this report are similar in appearance to those described after systemic administration of neurotoxin (Baumgarten and Bjorklund, 1976) and designer-drug (Molliver et al, 1990) induced degeneration of 5-HT fibers in rat brain. The dystrophic axons seen in the deep layers of FLD prefrontal cortex exhibited increased caliber, reduced branching, and swollen varicosities and resembled those seen after 5,7-DHT neurotoxin intracerebral injections into the 5-HT fibers-of-passage in MFB (Frankfurt and Azmitia, 1984) or cingulum bundle (Zhou and Azmitia, 1986). The 5-HTT fibers in DLBD and PD brains show degenerating fibers characterized by varicose swelling and clustering of fine terminals. This pattern of degeneration is seen in aged rats (van Luijtelaar et al, 1989) and S100B knockout animals

(un-published observation). The dystrophic axonal pattern suggests that these terminal fibers may be retracting from a region in which levels of trophic factor are reduced.

3.3. Possible Relevance of 5-HTT Axon Degeneration to Symptoms of Neurodegenerative Diseases

Dystrophic degenerative of serotonergic axons may contribute to the development of many of the symptoms of neurodegenerative diseases such as mood, motor, sensory, autonomic, cognitive, and sleep disorders (see Sandyk and Fisher 1988). In PD patients, selective 5-HT reuptake inhibitors (SSRIs) improve bradykinesia treated with L-dopa (Rampello et al, 2002). In our study, six of nine patients with neurodegenerative disease had histories of late-life depressive symptoms. Depression is believed to be a risk factor for the onset of Alzheimer's disease (Green et al, 2003; Chen et al, 1999; Kokmen et al, 1991; Kral and Emery, 1989). Affective disorders are often comorbid with neurodegenerative disorders that are associated with dementia (Allen and Burns, 1995; Schreinzer et al, 2004; Lauterbauch et al, 2004). Affective symptoms are frequently part of the initial presentation in neurodegenerative diseases (Ishihara and Brayne, 2006; Kessing and Anderson, 2004), and, in some cases, may be the dominant presenting symptoms (Ballard et al, 2002). A history of major depression, without specification of episode-related cognitive impairment, appears to be a risk factor for subsequent onset of dementia (Kessing and Andersen, 2004). This is supported by early work with twins, which found that depression and psychiatric illness were risk factors for developing dementia (Wetherell et al, 1999). Mood may be improved in depressed cognitively impaired older patients by treatment with antidepressants including selective serotonin reuptake inhibitors (SSRI) even in the absence of improvement in cognitive or motor domains (Schrag 2006; Ishihara and Brayne, 2006; Nebes et al, 2003). The actions of serotonin in the development and treatment of impairments seen in neurodegenerative diseases require further investigation (Gruden et al, 2007; Schmitt et al, 2006; Truchot et al, 2007).

Study Limitations—Although our findings demonstrated consistent differences in the extent and character of 5-HT axonal pathology in the nine neurodegenerative disease cases compared to the three control cases analyzed, the small size of the sample precluded a precise matching of the cases for age and postmortem interval. Recent unpublished work using 5-HTT immunostaining now includes 22 brains from neurologically typical normals, three of which are female, age range is 32–85 and average age is 57.2. No evidence of the frequent 5-HTT-specific axonal pathology reported here in the brains from neurodegenerative diseases is seen. The occasional 5-HTT-specific axonal pathology in the temporal cortical regions of neurologically normal subjects is confirmed (unpublished observation). Moreover, in contrast to the extensive neuropathological evaluation, the limited clinical characterization of the subjects in the study precluded a complete assessment of psychiatric history and medications in all cases. Nevertheless, these initial findings on 5HT fiber pathology in neurodegenerative diseases provide a strong rationale for more extensive analyses of the relationship between cognitive or affective parameters and 5-HT pathology in a larger cohort of clinically well characterized subjects.

4.0 EXPERIMENTAL PROCEDURES

4.1. Brains

Brains were obtained from the Harvard Brain Tissue Resource Center at McLean Hospital in Belmont, Massachusetts. We obtained 36 tissue blocks for our study from 12 brains, which met diagnostic criteria for the neurodegenerative diseases of Parkinson's disease (PD, n=3), Frontal Lobe Dementia (FLD, n=3), and Lewy Body Dementia (DLBD, n=3). The patients all met pre-mortem and postmortem criteria for the diagnosis made at Harvard Brain Tissue

Resource Center. The duration of the illness or specific treatments were not available from the records for all cases in this study. A majority of the patients with a neurodegenerative disorder also had a psychiatric history of depression (6/9), and in three cases, the information was unavailable and cannot be considered negative for depressive disorder. Neuropathologically normal brains (n=3) from donors with no medical or psychiatric history of illness were studied for comparison (Table 1).

4.2. Selection of Regions for Study

We used anterior brainstem blocks, which contained the substantia nigra and red nucleus, and the fiber tracts of the medial forebrain bundle, dorsal raphe cortical tract and the medial lemniscus. The temporal block we used contained the hippocampus (subiculum, CA fields and dentate gyrus) and the entorhinal cortex and associated white matter. The frontal block we used contained the dorsolateral prefrontal cortex (Brodmann layer 9) with all six cortical layers and a significant amount of the corpus callosum. We examined all layers of entorhinal and prefrontal cortices. In the hippocampus, we looked at the hilus of the dentate gyrus and the stratum radiatum of CA3 (paying particular note to the mossy fibers) and stratum radiatum of CA1. We also examined the fibers of the perforant path connecting the entorhinal cortex to CA1 and molecular layer of the dentate gyrus.

4.3. Orientation

We developed a method to produce a full section dark-field montage using a prototype condenser (Leitz Microscopic Company, Germany) for viewing with a 1.6X objective. Pictures were taken with a Kodak-6.0 million pixel camera (DCL 760). The montage of the various brain regions required between 6–25 images to assemble and were used to establish precise locations within the brain section.

4.4. Immunocytochemistry

Immunocytochemical studies were performed as previously described (Shivrba et al., 1998) using rabbit polyclonal antibodies raised against serotonin transporter (synthetic peptide from the carboxy-terminus (aa 602–622: GTLKERIIKSITPETPTEIPC) of the cloned rat serotonin transporter (AB177L, Calbiochem.). This site-specific antibody has been demonstrated to be highly selective for the 5-HTT proteins in immunocytochemistry and western analysis (Zhou et al, 1996; Qian et al, 1995). Dilutions of antibody were calculated to be in the linear range of staining intensity (1/1000–1/10,000 ab5-HTT). Brain tissue used for immunocytochemical analyses was immersion-fixed in cold 10% phosphate-buffered formalin (0.15 mol/L), pH 7.4. lmmunocytochemistry was performed by the avidin-biotin complex (ABC) method using Vectastain kits (Vector Labs, Inc., Burlingame, CA). Free-floating vibratome 50μm sections were treated for 30 min with 3% methanolic hydrogen peroxide to block non-specific endogenous peroxidase activity and rinsed in 0.05M Tris-buffered (pH 7.4) saline (TBS) containing 0.4% Triton X-100. The sections were treated for 30 min with 20% normal rabbit serum (NRS) to reduce non-specific background staining. Sections were then incubated in TBS with 1% NRS and 0.4% Trition x-100 with appropriate dilutions of primary antisera (AB-1, 1/5000) overnight at room temperature. The tissue was incubated first in biotinylated-secondary antibody (1:200 dilution) and subsequently in preformed ABC (90/d/10 ml avidin and 90;d/ml biotin). The final reaction was achieved by treating the sections with 0.02% hydrogen peroxide and DAB (0.5 mg/ml) in 0.1 M TBS, pH 7.4, for 5 min. Vibratome sections were mounted on gel-coated slides and air-dried following any immunocytochemical or histological procedures. All sections were dehydrated in a series of ethanol to xylene and coverslipped with Permount. Immunocytochemical controls consisted of either incubating tissue in non-immune sera or omitting incubation in primary antisera.

4.6. Morphometric Methods

Non-stereologic, morphometric measures of particle number and area were performed on each brain (n=3) for statistical analysis. Stereologic methods were not used because of the limited number of brain sections available, and the high density of 5-HTT-IR axons. The sections were viewed with a Leitz orthoplan microscope with Kohler illumination and photographed with a Nikon DCL760 digital camera for the analysis of 5-HTT-IR axonal number and area. Morphometric analysis was performed with the UTHSCSA Image Tool for windows (version 3.00) using pictures taken with a 25X PlFluotar Objective with 8X column magnification. At least three pictures were randomly taken in the prefronal cortical layers (II–VI) for each section from all groups. The photographs were untouched except for conversion into Grayscale before performing a threshold selection for illumination density measures of 5- HTT-IR labeling (setting of 150 on a 1–255 scale). All 5-HTT-IR labeled structures were automatically selected by the computer (10 pixel minimum cut-off) for counting, and measures of area. In the morphometric analysis of particles, normal varicosities were assumed from the images obtained to have an area $<10m^2$ profiles were estimated to have an area of between $30–75m^2$. The application of a stereologic method of analysis is precluded by the unavailability of representative sections throughout the entire dorsolateral prefrontal area.

4.7. Statistical Analysis

All values were transferred to Excel worksheet and averaged for each region from the four groups. To prepare histograms, the object area from each section was assigned to a bin of ascending area from 10–1500 μ^2, and the percentage of objects in each bin was calculated for each section, and then averaged for each group. ANOVA followed by student's t-test was performed and $p<.05$ used to establish significance. Histograms and statistical tests were carried out using the Data Analysis System on Microsoft Office XP Excel.

Study Limitations—Although our findings demonstrated consistent differences in the extent and character of 5-HT axonal pathology in the nine neurodegenerative disease cases compared to the three control cases analyzed, the small size of the sample precluded a precise matching of the cases for age and postmortem interval. Recent unpublished work using 5-HTT immunostaining now includes 22 brains from neurologically typical normals, three of which are female, age range is 32–85 and average age is 57.2. No evidence of the frequent 5-HTT-specific axonal pathology reported here in the brains from neurodegenerative diseases is seen. The occasional 5-HTT-specific axonal pathology in the temporal cortical regions of neurologically normal subjects is confirmed (unpublished observation). Moreover, in contrast to the extensive neuropathological evaluation, the limited clinical characterization of the subjects in the study precluded a complete assessment of psychiatric history and medications in all cases. Nevertheless, these initial findings on 5HT fiber pathology in neurodegenerative diseases provide a strong rationale for more extensive analyses of the relationship between cognitive or affective parameters and 5-HT pathology in a larger cohort of clinically well characterized subjects.

Acknowledgments

References

Abi-Dargham A, Gandelman MS, DeErausquin GA, Zea-Ponce Y, Zoghbi SS, Baldwin RM, Laruelle M, Charney DS, Hoffer PB, Neumeyer JL, Innis RB. SPECT imaging of dopamine transporters in human brain with iodine-123-fluoroalkyl analogs of beta-CIT. J. Nucl. Med. 1966; 37:1129–1133. [PubMed: 8965183]

Allen H, Burns A. The non-cognitive features of dementia. Rev. Clin. Gerontol. 1995; 5:57–75.

Aucoin J, Jiang P, Aznavour N, Tong XK, Buttini M, Descarries L, Hamel E. Selective cholinergic denervation, independent from oxidative stress, in a mouse model of Alzheimer's disease. Neuroscience. 2005; 132:73–86. [PubMed: 15780468]

Austin MC, Whitehead RE, Edgar CL, Janosky JE, Lewis DA. Localized decrease in serotonin transporter-immunoreactive axons in the prefrontal cortex of depressed subjects committing suicide. Neuroscience. 2002; 114:807–815. [PubMed: 12220580]

Azmitia E, Gannon P. The ultrastructural localization of serotonin immunoreactivity in myelinated and unmyelinated axons within the medial forebrain bundle of rat and monkey. J Neurosci. 1983; 3:2083–2090. [PubMed: 6604793]

Azmitia EC. The visualization and characterization of 5HT reuptake sites in the rodent and primate hippocampus. A preliminary study. J. Physiol. (Paris). 1981; 77:175–182. [PubMed: 7288636]

Azmitia EC, Liao B, Chen YS. Increase of tryptophan hydroxylase enzyme protein by dexamethasone in adrenalectomized rat midbrain. J. Neurosci. 1993; 13:5041–5055. [PubMed: 8254360]

Baker KG, Halliday GM, Hornung JP, Geffen LB, Cotton RG, Tork I. Distribution, morphology and number of monoamine-synthesizing and substance P-containing neurons in the human dorsal raphe nucleus. Neuroscience. 1991; 42:757–775. [PubMed: 1720227]

Ballard C, Johnson M, Piggott M, Perry R, O'Brien J, Rowan E, Perry E, Lantos P, Cairns N, Holmes C. A positive association between 5HT re-uptake binding sites and depression in dementia with Lewy bodies. J. Affect. Disord. 2002; 69:219–223. [PubMed: 12103469]

Baumgarten HG, Bjorklund A. Neurotoxic indoleamines and monoamine neurons. Annu. Rev. Pharmacol. Toxicol. 1976; 16:101–111. [PubMed: 779612]

Bossy-Wetzel E, Schwarzenbacher R, Lipton SA. Molecular pathways to neurodegeneration. Nat. Med. 2004; 10(Suppl):S2–S9. [PubMed: 15272266]

Castren E, Voikar V, Rantamaki T. Role of neurotrophic factors in depression. Curr. Opin. Pharmacol. 2007; 7:18–21. [PubMed: 17049922]

Chen P, Ganguli M, Mulsant BH, DeKosky ST. The temporal relationship between depressive symptoms and dementia: a community-based prospective study. Arch. Gen. Psychiatry. 1999; 56:261–266. [PubMed: 10078504]

Chinaglia G, Landwehrmeyer B, Probst A, Palacios JM. Serotoninergic terminal transporters are differentially affected in Parkinson's disease and progressive supranuclear palsy: an autoradiographic study with [3H]citalopram. Neuroscience. 1993; 54:691–699. [PubMed: 8332256]

Craven RM, Priddle TH, Cooper SJ, Crow TJ, Esiri MM. The dorsal raphe nucleus in schizophrenia: a post mortem study of 5-hydroxytryptamine neurones. Neuropathol. Appl. Neurobiol. 2005; 31:258–269. [PubMed: 15885063]

Descarries L, Beaudet A, Watkins KC. Serotonin nerve terminals in adult rat neocortex. Brain Res. 1975; 100:563–588. [PubMed: 1192194]

Dickson DW, Schmidt ML, Lee VM, Zhao ML, Yen SH, Trojanowski JQ. Immunoreactivity profile of hippocampal CA2/3 neurites in diffuse Lewy body disease. Acta Neuropathol. (Berl). 1994; 87:269–276. [PubMed: 7912027]

Frankfurt M, Azmitia EC. The effect of intracerebral injections of 5,7-dihydroxytryptamine and 6-hydroxydopamine on the serotonin-immunoreactive cell bodies and fibers in the adult rat hypothalamus. Brain Res. 1983; 261:91–99. [PubMed: 6404500]

Frankfurt M, Azmitia EC. Regeneration of serotonergic fibers in the rat hypothalamus following unilateral 5,7-dihydroxytryptamine injection. Brain Res. 1984; 298:273–282. [PubMed: 6609746]

Fuxe K. Evidence for the existence of monoamine neurons in the central nervous system. IV. The distribution of monoamine terminals in the central nervous system. Acta Physiol. Stand. 1965; 64(Suppl. 247):41–85.

Green RC, Cupples LA, Kurz A, Auerbach S, Go R, Sadovnick D, Duara R, Kukull WA, Chui H, Edeki T, Griffith PA, Friedland RP, Bachman D, Farrer L. Depression as a risk factor for Alzheimer disease: the MIRAGE Study. Arch Neurol. 2003; 60:753–759. [PubMed: 12756140]

Gruden MA, Davidova TB, Malisauskas M, Sewell RD, Voskresenskaya NI, Wilhelm K, Elistratova EI, Sherstnev VV, Morozova-Roche LA. Differential neuroimmune markers to the onset of Alzheimer's disease neurodegeneration and dementia: autoantibodies to Abeta((25–35)) oligomers, S100b and neurotransmitters. J. Neuroimmunol. 2007; 186:181–192. [PubMed: 17477976]

Halliday GM, Blumbergs PC, Cotton RG, Blessing WW, Geffen LB. Loss of brainstem serotonin- and substance P-containing neurons in Parkinson's disease. Brain Res. 1990; 510:104–107. [PubMed: 1691042]

Haan EA, Jennings IG, Cuello AC, Nakata H, Fujisawa H, Chow CW, Kushinsky R, Brittingham J, Cotton RG. Identification of serotonergic neurons in human brain by a monoclonal antibody binding to all three aromatic amino acid hydroxylases. Brain Res. 1987; 426:19–27. [PubMed: 2891407]

Haglund M, Sjobeck M, Englund E. Locus ceruleus degeneration is ubiquitous in Alzheimer's disease: possible implications for diagnosis and treatment. Neuropathology. 2006; 26:528–532. [PubMed: 17203588]

Ishihara L, Brayne C. What is the evidence for a premorbid parkinsonian personality: a systematic review. Movement Disorders. 2006; 21:1066–1072. [PubMed: 16755553]

Kertesz A. Pick Complex: an integrative approach to frontotemporal dementia: primary progressive aphasia, corticobasal degeneration, and progressive supranuclear palsy. Neurologist. 2003; 9:311–317. [PubMed: 14629785]

Kessing LV, Andersen PK. Does the risk of developing dementia increase with the number of episodes in patients with depressive disorder and in patients with bipolar disorder? J Neurol. Neurosurg. Psychiatry. 2004; 75:1662–1666. [PubMed: 15548477]

Kokmen E, Beard CM, Chandra V, Offord KP, Schoenberg BS, Ballard DJ. Clinical risk factors for Alzheimer's disease: a population-based case-control study. Neurology. 1991; 41:1393–1397. [PubMed: 1891088]

Kral VA, Emery OB. Long-term follow-up of depressive pseudodementia of the aged. Can J Psychiatry. 1989; 34:445–446. [PubMed: 2766198]

Kung L, Force M, Chute DJ, Roberts RC. Immunocytochemical localization of tyrosine hydroxylase in the human striatum: a postmortem ultrastructural study. J. Comp. Neurol. 1998; 390:52–62. [PubMed: 9456175]

Langlais PJ, Thal L, Hansen L, Galasko D, Alford M, Masliah E. Neurotransmitters in basal ganglia and cortex of Alzheimer's disease with and without Lewy bodies. Neurology. 1993; 43:1927–1934. [PubMed: 8105420]

Lauterbach EC, Freeman A, Vogel RL. Differential DSM-III psychiatric disorder prevalence profiles in dystonia and Parkinson's disease. J. Neuropsychiatry Clin. Neurosci. 2004; 16:29–36. [PubMed: 14990756]

Liu Y, Nakamura S. Stress-induced plasticity of monoamine axons. Front. Biosci. 2006; 11:1794–1801. [PubMed: 16368556]

Marksteiner J, Walch T, Bodner T, Gurka P, Donnemiller E. Fluoxetine in Alzheimer's disease with severe obsessive compulsive symptoms and a low density of serotonin transporter sites. Pharmacopsychiatry. 2003; 36:207–209. [PubMed: 14571357]

Menza MA, Palermo B, DiPaola R, Sage JI, Ricketts MH. Depression and anxiety in Parkinson's disease: possible effect of genetic variation in the serotonin transporter. J Geriatr Psychiatry Neurol. 1999; 12:49–52. [PubMed: 10483924]

Molliver DC, Molliver ME. Anatomic evidence for a neurotoxic effect of (+/−)-fenfluramine upon serotonergic projections in the rat. Brain Res. 1990; 511:165–168. [PubMed: 2331614]

Molliver ME. Serotonergic neuronal systems: what their anatomic organization tells us about function. J. Clin. Psychopharmacol. 1987; 7(6 Suppl):3S–23S. [PubMed: 3323265]

Nebes RD, Pollock BG, Houck PR, Butters MA, Mulsant BH, Zmuda MD, Reynolds CF 3rd. Persistence of cognitive impairment in geriatric patients following antidepressant treatment: a randomized, double-blind clinical trial with nortriptyline and paroxetine. J. Psychiatr. Res. 2003; 37:99–108. [PubMed: 12842163]

Ohara K, Kondo N, Ohara K. Changes of monoamines in post-mortem brains from patients with diffuse Lewy body disease. Prog Neuropsychopharmacol Biol Psychiatry. 1998; 22:311–317. [PubMed: 9608603]

O'Hearn E, Battaglia G, De Souza EB, Kuhar MJ, Molliver M. Methylenedioxy amphetamine (MDA) and methylenedioxymethamphetamine (MDMA) cause selective ablation of serotonergic axon terminals in forebrain: immunocytochemical evidence for neurotoxicity. J. Neurosci. 1988; 8:2788–2803. [PubMed: 2457659]

Perry EK, Irving D, Kerwin JM, McKeith IG, Thompson P, Collerton D, Fairbairn AF, Ince PG, Morris CM, Cheng AV, et al. Cholinergic transmitter and neurotrophic activities in Lewy body dementia: similarity to Parkinson's and distinction from Alzheimer disease. Alzheimer. Dis. Assoc. Disord. 1993; 7:69–79. [PubMed: 8347330]

Qian Y, Melikian HE, Rye DB, Levey AI, Blakely RD. Identification and characterization of antidepressant-sensitive serotonin transporter proteins using site-specific antibodies. J Neurosci. 1995; 15(2):1261–1274. [PubMed: 7869097]

Rampello L, Chiechio S, Raffaele R, Vecchio I, Nicoletti F. The SSRI, citalopram, improves bradykinesia in patients with Parkinson's disease treated with L-dopa. Clin Neuropharmacol. 2002; 25(1):21–24. [PubMed: 11852292]

Sandyk R, Fisher H. Serotonin in involuntary movement disorders. Int. J. Neurosci. 1988; 42:185–208. [PubMed: 3061953]

Schmitt JA, Wingen M, Ramaekers JG, Evers EA, Riedel WJ. Serotonin and human cognitive performance. Curr Pharm Des. 2006; 12:2473–2486. [PubMed: 16842171]

Schreinzer D, Ballaban T, Brannath W, Lang T, Hilger E, Fasching P, Fischer P. Components of behavioral pathology in dementia. Int. J. Geriatr. Psychiatry. 2005; 20:137–145. [PubMed: 15660411]

Schrag A. Quality of life and depression in Parkinson's disease. J. Neurological Sci. 2006; 248:151–157.

Shiurba RA, Spooner ET, Ishiguro K, Takahashi M, Yoshida R, Wheelock TR, Imahori K, Cataldo AM, Nixon RA. Immunocytochemistry of formalin-fixed human brain tissues: microwave irradiation of free-floating sections. Brain Res. Brain Res. Protoc. 1998; 2:109–119. [PubMed: 9473616]

Sparks DL, Markesbery WR. Altered serotonergic and cholinergic synaptic markers in Pick's disease. Arch. Neurol. 1991; 48:796–799. [PubMed: 1898253]

Steinbusch HW. Distribution of serotonin-immunoreactivity in the central nervous system of the rat-cell bodies and terminals. Neuroscience. 1981; 6:557–618. [PubMed: 7017455]

Stout SS, Somerset WI, Miller A, Musselman DL. Paroxetine use in medically ill patients. Psychopharmacol. Bull. 2003; 37(Suppl 1):108–122. [PubMed: 14566206]

Szabo Z, Kao PF, Mathews WB, Ravert HT, Musachio JL, Scheffel U, Dannals RF. Positron emission tomography of 5-HT reuptake sites in the human brain with C-11 McN5652 extraction of characteristic images by artificial neural network analysis. Behav. Brain Res. 1996; 73:221–224. [PubMed: 8788506]

Truchot L, Costes SN, Zimmer L, Laurent B, Le Bars D, Thomas-Anterion C, Croisile B, Mercier B, Hermier M, Vighetto A, Krolak-Salmon P. Up-regulation of hippocampal serotonin metabolism in mild cognitive impairment. Neurology. 2007; 69:1012–1017. [PubMed: 17785670]

Underwood MD, Khaibulina AA, Ellis SP, Moran A, Rice PM, Mann JJ, Arango V. Morphometry of the dorsal raphe nucleus serotonergic neurons in suicide victims. Biol. Psychiatry. 1999; 46:473–483. [PubMed: 10459396]

van Luijtelaar MG, Steinbusch HW, Tonnaer JA. Similarities between aberrant serotonergic fibers in the aged and 5,7-DHT denervated young adult rat brain. Exp. Brain Res. 1989; 78:81–89. [PubMed: 2591520]

Varnas K, Halldin C, Hall H. Autoradiographic distribution of serotonin transporters and receptor subtypes in human brain. Hum. Brain Mapp. 2004; 22:246–260. [PubMed: 15195291]

Wetherell JL, Gatz M, Johansson B, Pedersen NL. History of depression and other psychiatric illness as risk factors for Alzheimer disease in a twin sample. Alzheimer Dis. Assoc. Disord. 1999; 13:47–52. [PubMed: 10192642]

Wiklund L, Bjorklund A. Mechanisms of regrowth in the bulbospinal serotonin system following 5,6-dihydroxytryptamine induced axotomy. II. Fluorescence histochemical observations. Brain Res. 1980; 191:109–127.

Zhou FC, Azmitia EC. Induced homotypic sprouting of serotonergic fibers in hippocampus. II. An immunocytochemistry study. Brain Res. 1986; 373:337–348. [PubMed: 3013362]

Zhou FC, Bledsoe S, Lumeng L, Li TK. Reduced serotonergic immunoreactive fibers in the forebrain of alcohol-preferring rats. Alcohol Clin. Exp. Res. 1994; 18:571–579. [PubMed: 7943657]

Zhou FC, Xu Y, Bledsoe S, Lin R, Kelley MR. Serotonin transporter antibodies: production, characterization, and localization in the brain. Brain Res. Mol. Brain Res. 1996; 43:267–278. [PubMed: 9037542]

Substantia Nigra/Midbrain   Hippocampus/Entorhinal   Prefrontal Cortex
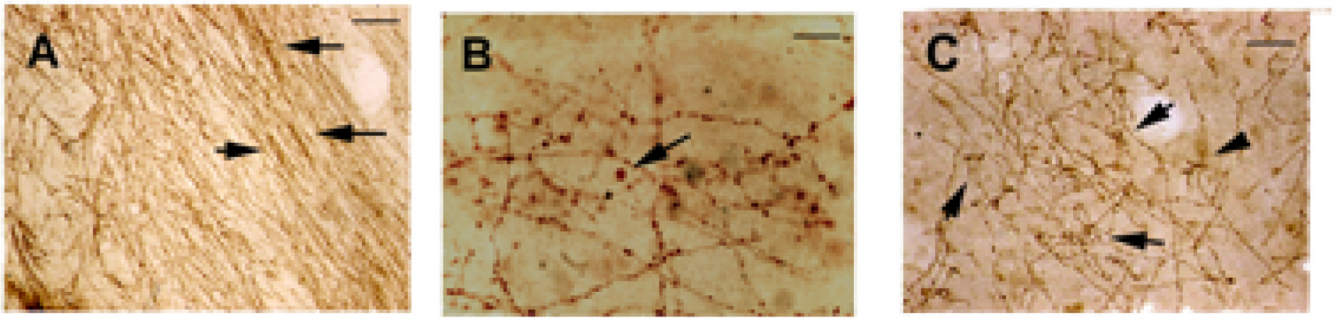
Figure 1. 5-HTT-IR axons in control brain

5-HTT-IR axons are seen in brains from control individuals. A. In the midbrain/substantia nigra sections heavy fiber labeling is seen in the medial lemniscal with the fibers throughout the entire pathway. These fibers of passage have small varicosities and often form tight bundles (arrows). Scale bar is 200μm. B. In the hippocampus and entorhinal areas the 5-HTT-IR axons are forming terminal boutons. In these sections larger boutons can be seen (arrow). Scale bar is 50μm. C. In the prefrontal cortex, the 5-HTT-IR fibers form clusters around cell bodies in pyramidal layers (arrows). Scale bar is 200μm.
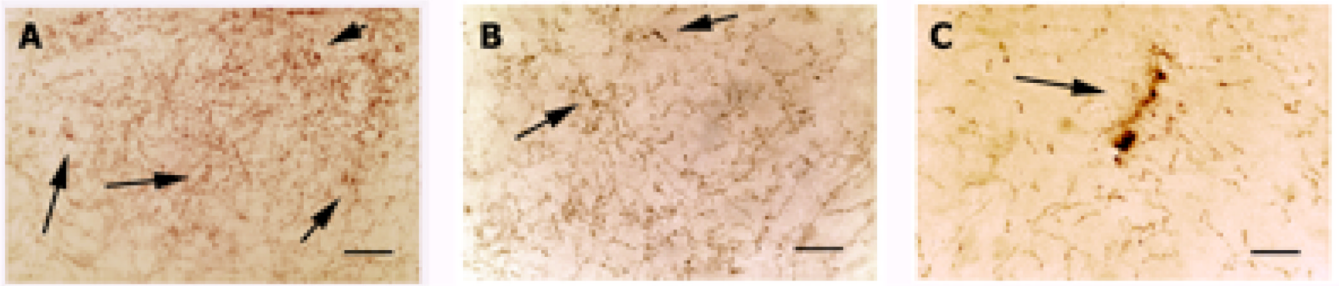
Figure 2. Rare 5-HTT-IT axons in a control 79 year old brain
Dystrophic 5-HTT-IR axons are seen, but infrequently, in the brain of a control 79-year-old-male. A. Layer III of entorhinal cortex is heavily innervated with 5-HTT-IR axons. Among the normal fibers, abnormal fibers can be seen forming dense clusters, which can condense into a larger degenerating profile (arrows). B. In the polymorphic area of the DG abnormally large varicosities can be found (arrow). C. In the dendritic region of CA3 degenerating profiles are seen among normal fibers. Scale bar is 50μm in all panels.
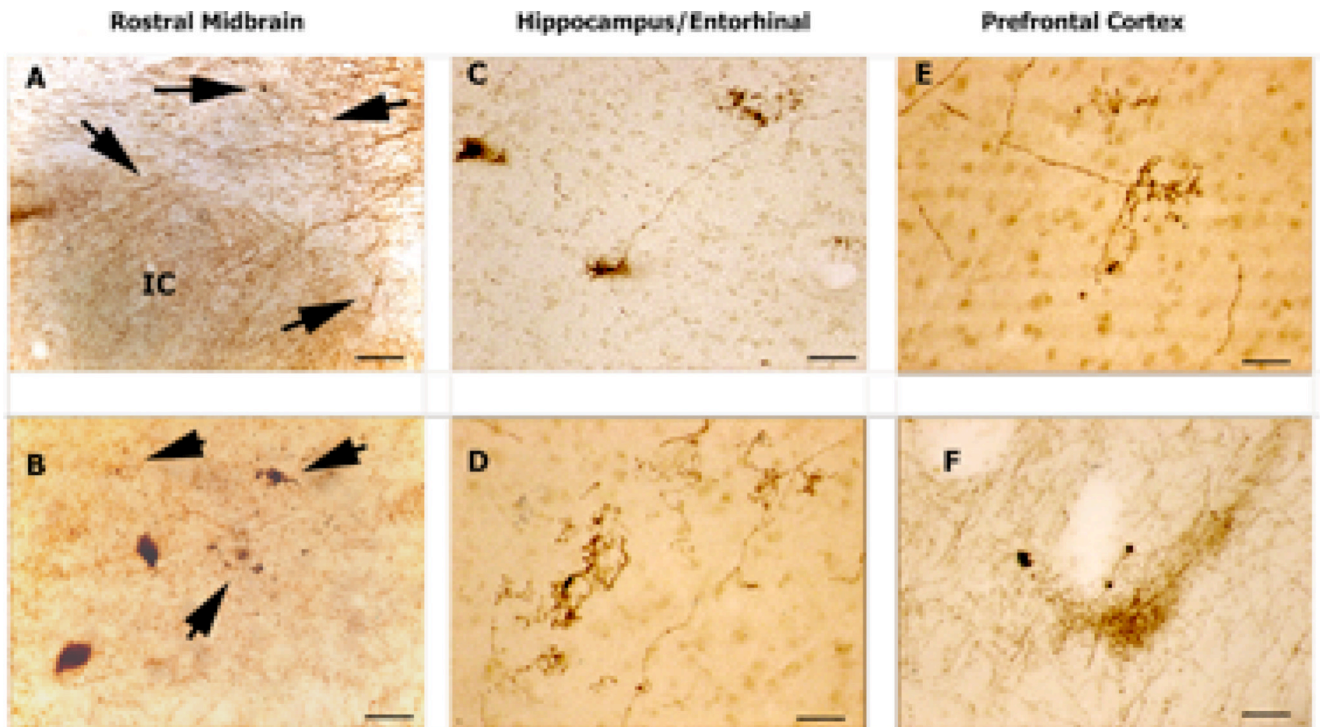
Figure 3. 5-HTT-IR Axons in Diffuse Lewy Body Brain
5-HTT-IR axons in brains from patients diagnosed with Diffuse Lewy-Body Dementia. A. This picture shows normal appearing 5-HTT-IR axonal bundles in the dorsal aspect of the section just above the inferior colliculus (IC). There is evidence of dystrophic 5-HTT-IR axons in the fiber bundles (arrows). Scale bar is 200μm. B. Normal and abnormal (arrows) terminals in the substantia nigra. Two pigmented nigra neurons can be seen. Scale bar is 50μm. C. Splayed 5-HTT-IR terminals seen in CA3 dendritic region. Scale bar is 50μm. D. Tight clusters of 5-HTT-IR axons in Layer III of entorhinal cortex. The number of labeled fibers is reduced in this region. Scale bar is 50μm. E. Tight cluster of 5-HTT-IR fibers in Layer III of prefrontal cortex. Scale bar is 50μm. F. In deep layers of cortex, aggregates of fibers are found among dystrophic 5-HTT-IR axons with enlarged varicosities. Scale bar is 200μm.

**Rostral Midbrain**   **Hipppocampus/Entorhinal**   **Prefrontal Cortex**
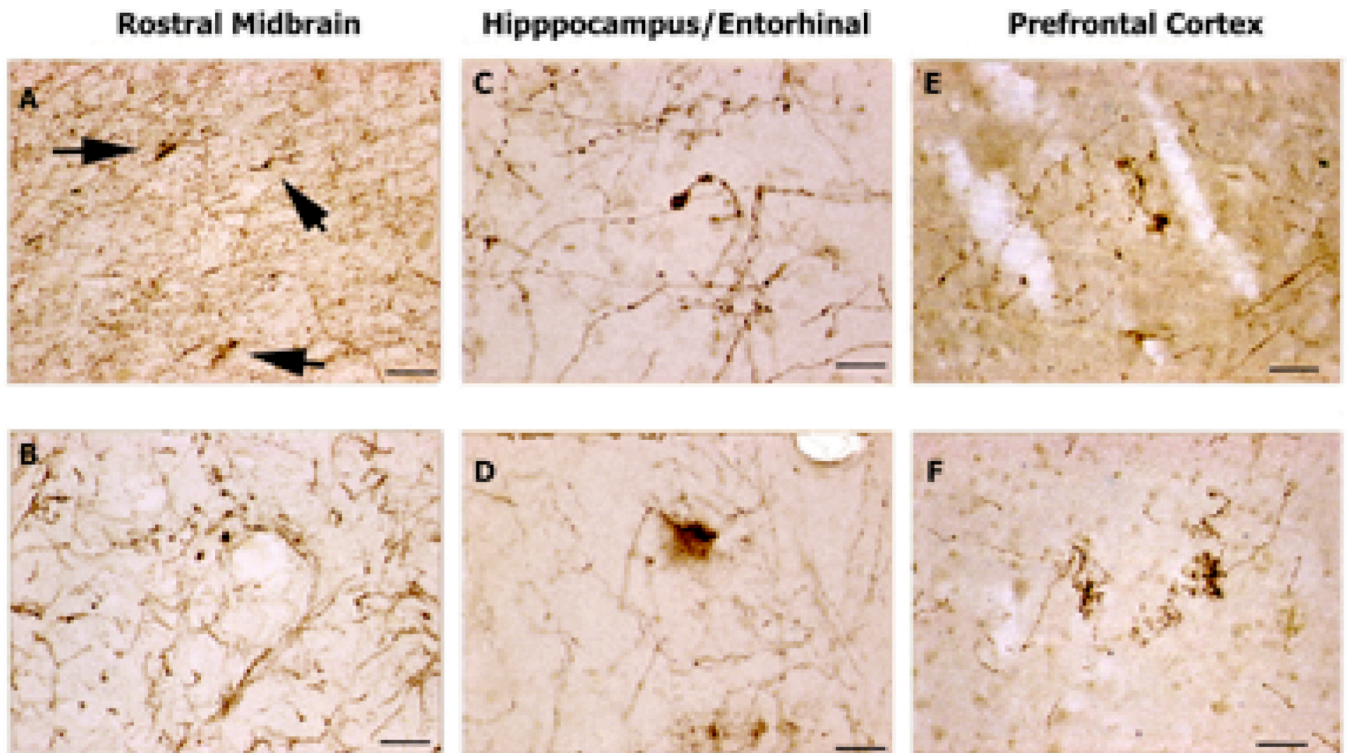
Figure 4. 5-HTT-IR Axons in Parkinson' Disease Donor Brain
5-HTT-IR axons in brains from patients diagnosed with Parkinson's disease. A. 5-HTT-IR
axons in the red nucleus show some abnormal fibers (arrows) among many normal fibers.
Scale bar is 200μm. B. In midline areas 5-HTT-IR fibers with enlarged varicosities are
found among normal fibers. Scale bar is 50μm. C. Dystrophic 5-HTT-IR axons with
enlarged varicosity in the dendritic regions of CA1. Scale bar is 50μm. D. Dystrophic 5-
HTT-IR axons are splayed and degenerating in the upper layers of the entorhinal cortex.
Scale bar is 50μm. E. Fine degenerating 5-HTT-IR axons in the upper layer of prefrontal
cortex. Scale bar is 50μm. F. Fine, dense clusters of 5-HTT-IR axons in the deeper layers of
prefrontal cortex. Scale bar is 50μm.
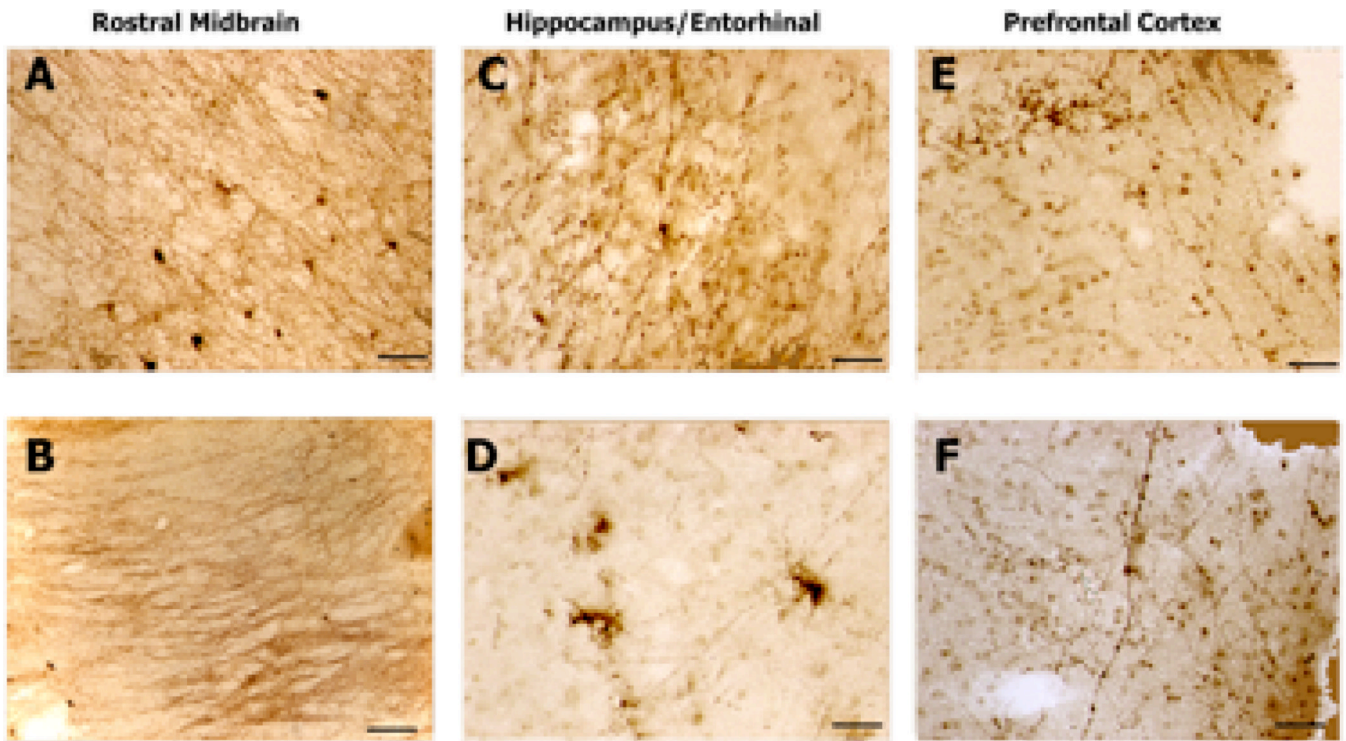
Figure 5. 5-HTT-IR Axons in Frontal Lobe Dementia
5-HTT-IR axons in brains from patients diagnosed with Frontal Lobe Dementia. A. Dense innervation by 5-HTT-IR fibers is seen in the substantia nigra nucleus. No dystrophic 5-HTT-IR fibers seen. Scale bar is 200μm. B. Heavy labeling of the fibers in the medial lemniscal tract. No dystrophic 5-HTT-IR fibers seen. Scale bar is 200μm. C. Enlarged varicosities seen in hilus area of dentate gyrus. Scale bar is 50μm. D. Several splayed and degenerating 5-HTT-IR terminals seen in the upper layer of entorhinal cortex. Note reduced appearance of normal 5-HTT-IR fibers. Scale bar is 50μm. E. Dense clustering and aggregation of 5-HTT-IR axons in layer II–III of the prefrontal cortex. Note normal tangential fibers in layer I. Scale bar is 50μm. F. Enlarged 5-HTT-IR axons are seen in the deeper layers of prefrontal cortex. 5-HTT-IR axonal innervation appears reduced from normal. Scale bar is 50μm.
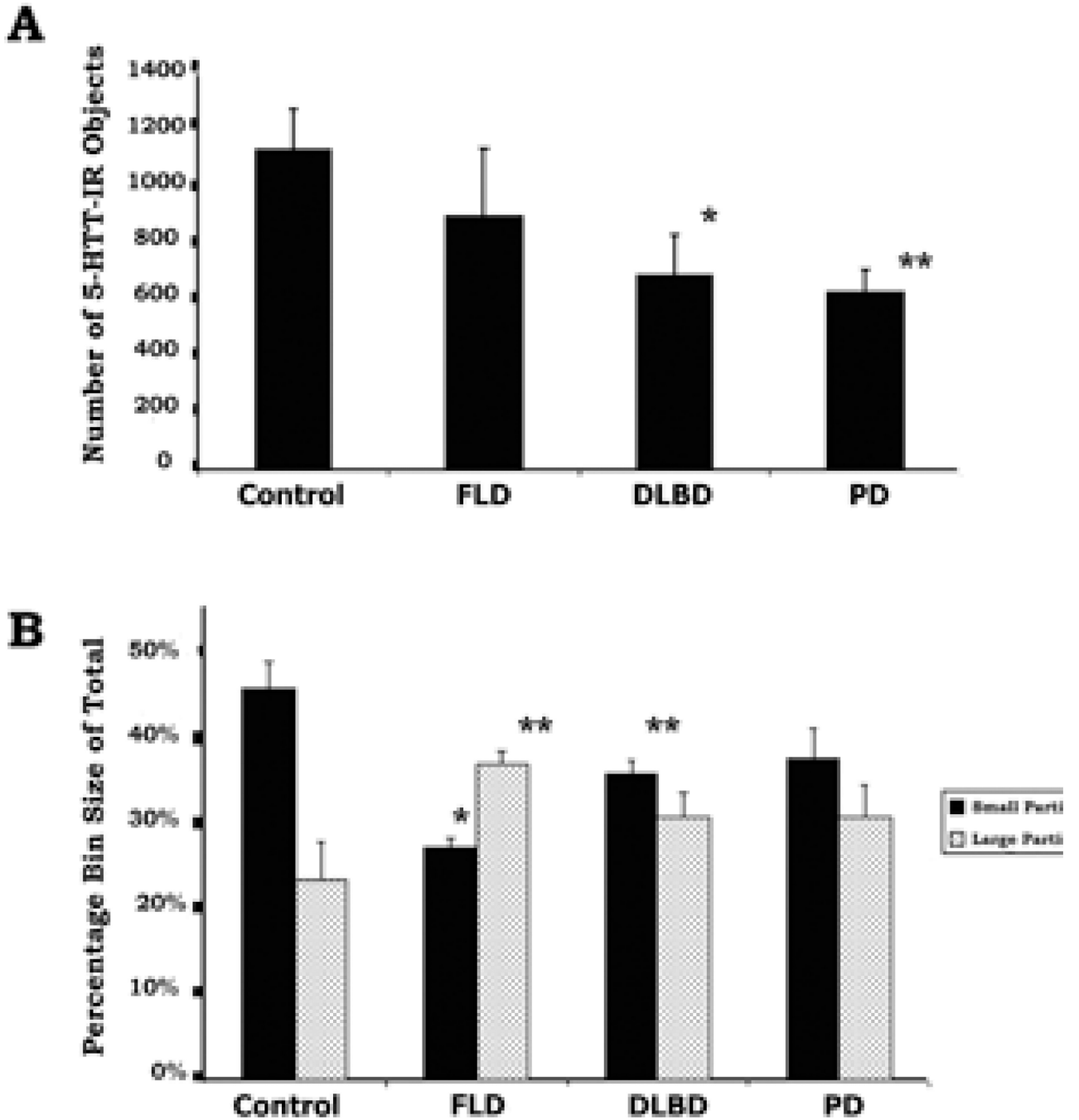
Figure 6. Morphometric Analysis of 5-HTT-IR in Prefrontal Cortex
This figure shows the results from morphometric analysis of the labeled objects found in
prefrontal cortex of control and diseased brains using threshold setting of immunoreactive
density. A. The total number of particles (varicosities, fibers and degenerating axons) was
counted in an area of $0.5mm^2$ in layer III–V of the cortex. Each bar is the mean of three
brains from each group (see Materials and Methods for details). The number of particles
selected was lower for all diseased-groups compared to normal prefrontal cortex, and was
significant for the DLBD and PD. B. A histogram of all particle areas was made form the
particles selected for part A. The percentage of the total number of particles which had the
smallest area ($<10\mu^2$) is shown in the black bars (average ± SEM) with an n=3 for all

groups. The larger objects (30–75μ2) are shown in stipple. The brains from controls had a higher percentage of particles having a smaller area (varicosities and fine axons) when compared to the brains from diseased cases. By contrast, the brains from diseased cases had significantly higher percentage of particles having a larger area (large axons and degenerating profiles). *=p<.05; **=p<.01.
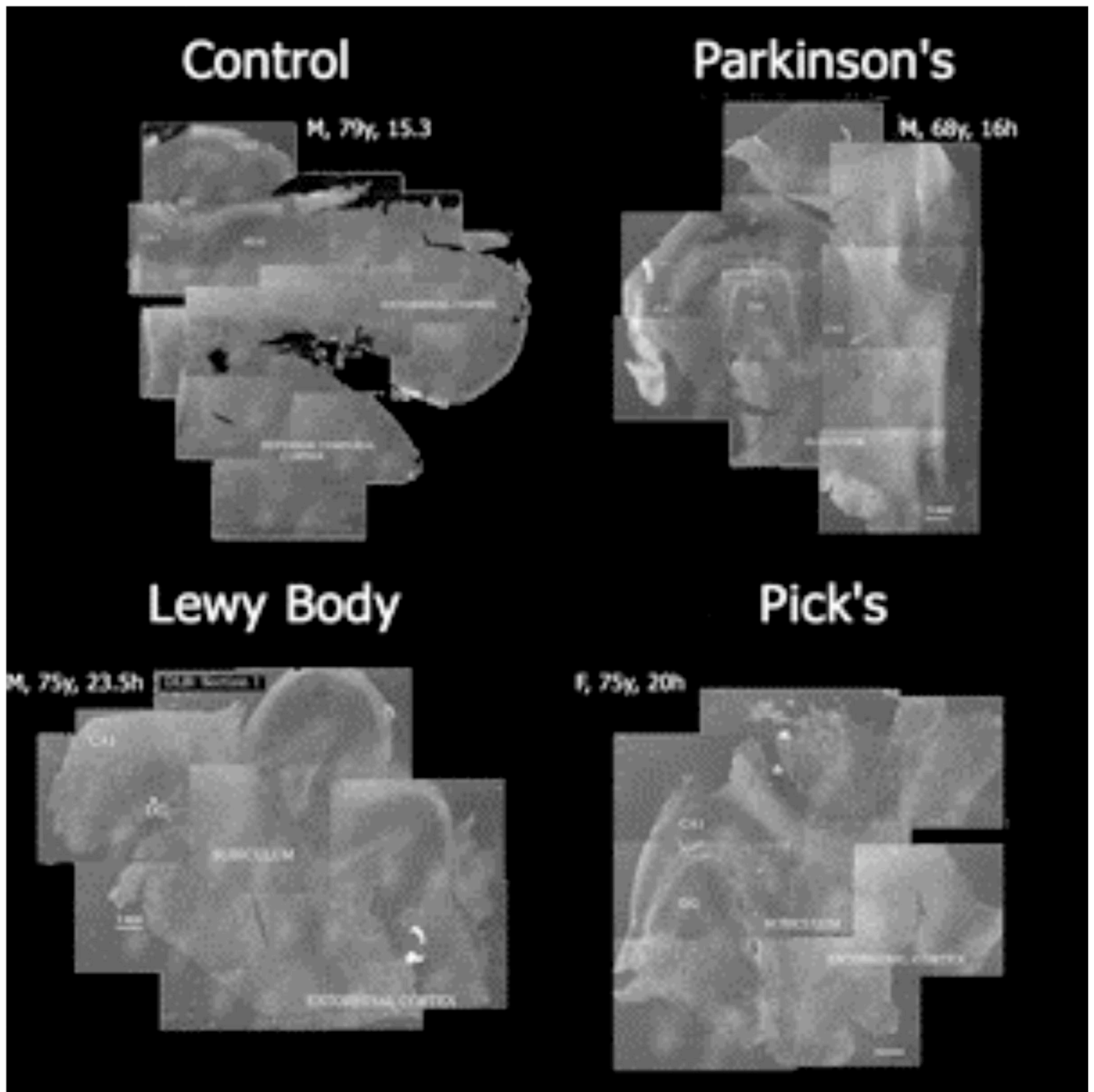
Figure 7. Dark field Montage

Table 1

The Diagnosis, Demographic, Postmortem Interval (PMI) History of Depression and Antidepressant Treatment

Brain #	Diagnosis	Gender	Age	PMI	Depression	Antidepressant Treatment
B2374	None	M	72	8.5	-	-
B2469	None	F	54	3.5	-	-
B3573	None	M	79	15.3	-	-
B4426	DLBD	M	75	23.5	+	-
B4866	DLBD	M	67	14.85	+	-
B5085	DLBD	M	68	5.5	+	+
B4927	FLD	F	68	14.33	+	+
B5007	FLD	F	72	6.58	N/A	N/A
B5035	FLD	F	75	20	+	+
B4934	PD	M	68	17.16	N/A	N/A
B5207	PD	M	64	18.58	N/A	N/A
B5227	PD	M	77	26	+	+